van der Waals Complex of Dimethyl Ether with Carbon Dioxide

P. Van Ginderen, W. A. Herrebout, and B. J. van der Veken*

Department of Chemistry, University of Antwerp (RUCA), Groenenborgerlaan 171, B2020 Antwerpen, Belgium

Received: March 4, 2003; In Final Form: May 16, 2003

The 1:1 complex between dimethyl ether and carbon dioxide was studied experimentally in solutions in liquid argon, using infrared spectroscopy, and theoretically, using ab initio calculations at the MP2/6-311++G(d,p) level. The complex is formed through the interaction of the dimethyl ether oxygen atom with the CO_2 carbon atom, with the CO_2 perpendicular to the 2-fold axis of dimethyl ether, in the plane of the heavy atoms of the latter. Observed vibrational bands are in good agreement with the predicted vibrational frequencies. The standard complexation enthalpy of the complex in liquid argon was determined from a temperature dependent study of the spectra and was found to be $-8.0(3)$ kJ mol^{-1}. Some aspects of the Fermi resonance between the symmetric stretch and the first overtones of the two bending modes of the CO_2 moiety of the complex are discussed.

Introduction

Since the first spectroscopic investigation of the interaction of carbon dioxide with the simplest oxygen donor, i.e., water,[1,2] the interest in such complexes has not waned, with the research efforts being spurred by, among others, the urge to gain insight into the more fundamental aspects of the Lewis acid/base interaction[3−6] or by the need to understand the solubility of organic compounds when supercritical CO_2 is used as a green-chemistry solvent.[7−10]

A variety of experimental techniques have been used to study the complexes of CO_2 with several oxygen donors in the vapor[3,4,6,8] and liquid phase[11,12] and in low-temperature matrixes,[1,2,13−16] whereas also considerable theoretical attention was devoted to them, mainly using ab initio methods.[9,10,17−22] The experimental studies have supplied a wealth of information on the complexes studied but have up to now failed to yield direct experimental results on their stability, with the only data available in the literature having been derived by the ab initio studies. As the stability of a compound is a fundamental property that is of high importance for its chemistry, we have embarked on a study of CO_2 complexes as formed in cryosolutions, using liquid argon (LAr) as the solvent. In these solutions, the complexes are formed under equilibrium conditions, so that their stability can be determined. In this study, we report on the infrared spectra of the complex CO_2 forms with dimethyl ether (DME) and on ab initio calculations of its structure and vibrational frequencies. In the paragraphs below, we will show that a 1:1 complex has been observed and that its stability, under the form of a standard complexation enthalpy $\Delta H°$, could be determined. We also report on the Fermi resonance between the first overtones of the CO_2 bendings and the CO_2 symmetric stretch, which over the past decades has been thoroughly studied for monomeric CO_2 in the gas and solid phases and for CO_2 adsorbed to surfaces but for which in weak complexes to our best knowledge no experimental data have been presented before.

* To whom correspondence should be addressed.

Experimental Section

The sample of dimethyl ether was obtained commercially (Aldrich Chem. Co. 29,529-9) and was used without further purification. CO_2 in natural isotopic abundance was synthesized in small amounts by the reaction of Na_2CO_3 (Aldrich Chem. Co. 20,442-0) with anhydrous H_2SO_4 (Acros Organics C.A.S. 7664-93-9). The crude CO_2 was purified by slowly pumping the gas through a U-tube kept at 165 K in a cold slush. By using $Na_2{}^{13}CO_3$ (Aldrich Chem. Co. 49,076-8) in a similar procedure, $^{13}CO_2$ was also synthesized. The argon used has a stated purity of 99.999 9% and was used without further purification.

The infrared spectra were recorded on a Bruker IFS 66v Fourier transform spectrometer, using a Globar source in combination with a Ge/KBr beam splitter and a broadband MCT detector. In general, the interferograms were averaged over 300 scans, Happ Genzel apodized, and Fourier transformed using a zero-filling factor of 4 to yield spectra at a resolution of 0.5 cm^{-1}. For the study of the Fermi resonance, spectra were recorded at 0.1 cm^{-1} resolution, with the interferograms being averaged over 1000 scans.

A detailed description of the liquid noble gas setup was given previously.[23] Liquid cells with path lengths of 1 and 7 cm, equipped with wedged silicon and wedged ZnSe, respectively, were used to record the spectra.

Computational Details. Theoretical information on the geometry of the 1:1 complex and on its vibrational frequencies was obtained by carrying out ab initio calculations, at the MP2/6-311++G(d,p) level. During the geometry optimizations and the harmonic force field calculation, corrections for BSSE were taken into account explicitly using the CP-corrected gradient techniques developed by Simon et al.[24] To reduce the computational cost, the cubic force field was calculated at the somewhat lower MP2/6-31G(d) level, which is justified by the weaker basis set dependence of cubic force fields and by the fact that at both levels completely similar structures were obtained for the complex, the van der Waals bond length between the DME oxygen and the CO_2 carbon differing by less than 5×10^{-3} Å. All ab initio calculations were performed using Gaussian 98.[25]

10.1021/jp034553i CCC: $25.00
Published on Web 06/24/2003

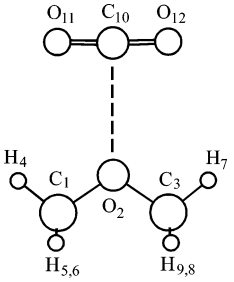

Figure 1. Projection in the DME heavy atom plane of the structure of the 1:1 complex of DME with CO_2.

Solvation Gibbs energies of monomers and complexes were obtained from Monte Carlo perturbation calculations, using a modified version of BOSS 4.1.[26] All simulations were run in the NPT ensemble, using periodic boundary conditions. The system consisted of one solute molecule surrounded by 256 solvent atoms. Preferential Metropolis sampling was used as described before.[27] An attempt to move the solute molecule was made on every 50th configuration, and a change in volume was tried on every 600th configuration. The ranges for the attempted moves were the same in each calculation and provided a ~40% acceptance probability for new configurations. The path for $\lambda = 0$ (pure argon) to $\lambda = 1$ (a solution with one solute molecule) was completed in 40 equidistant steps. Each step consisted of an equilibrium phase for 20.0×10^6 configurations, followed by a production phase of 50.0×10^6 configurations. The Gibbs energy changes between the perturbed and reference systems were always small enough ($\approx kT$) to guarantee reliable results by the statistical pertubation theory.

The enthalpy of solvation $\Delta_{sol}H$ and the entropy of solvation $\Delta_{sol}S$ in LAr were extracted from the Gibbs energies of solvation $\Delta_{sol}G$, using a method similar to that described by Levy et al.[28] To this end, for each species, the Gibbs energies of solvation were calculated at 10 different temperatures between 88 and 138 K, at a pressure of 28.2 bar, i.e., the vapor pressure of LAr at 138 K.

Results and Discussion

Ab Initio Calculations. Structure optimizations starting from different relative orientations of dimethyl ether with respect to CO_2 consistently converged to the same complex. In this, the C_{2v} symmetry of DME is preserved, with the CO_2 molecule situated perpendicular to the 2-fold axis, in the DME heavy atom plane. The projection of the structure in this plane is shown in Figure 1, whereas the structural data have been collected in Table 1.

The van der Waals bond length, defined as the distance between O(2) and C(10) equals 2.812 Å. This is slightly shorter than the value of 2.886 Å resulting from the ab initio calculation at the same level on $H_2O{\cdot}CO_2$, which is in reasonable agreement with the experimental bond length of 2.836 Å derived from microwave experiments on that complex.[5] The main structural change in DME upon complexation is the lengthening of the C−O bonds by 1.9×10^{-3} Å, with smaller changes in the C−H bond lengths and with minor changes in the interbond angles. Upon complexation, CO_2 loses its strict linearity, resulting in a valence angle of 178.1 degrees, with the oxygen atoms shifted away from the DME moiety. The C═O bond lengths are slightly shorter in the complex than in the monomer, by 0.2×10^{-4} Å.

The basis set used for the structure optimizations is somewhat limited, which may lead to less satisfactory energies. Therefore, based on previous experience,[29] the energies for the monomers and the complex were also calculated from single point calculations, at the MP2/6-311++G(2p,2d) and the MP2/6-311++G(3df,2pd) level, using the MP2/6-311++G(d,p) optimized structures. The complexation energies, calculated from these in the supermolecule approximation, are −13.06 kJ mol^{-1} (MP2/6-311G(d,p), −13.83 kJ mol^{-1} (MP2/6-311++G(2d,2p), and −15.58 kJ mol^{-1} (MP2/6-311++G(3df,2pd). These values indicate that the complex is weak but well within the reach of a cryosolutions investigation.[30]

The harmonic vibrational frequencies and infrared intensities calculated for monomer dimethyl ether and carbon dioxide and for the 1:1 complex have been collected in Table 2. The symmetry species indicated are those of the complex. It can

TABLE 1: MP2/6-311++G(d,p) Structural Parameters[a] for DME, CO_2, and DME·CO_2

parameters	DME	CO_2	DME·CO_2
$R(C_1-O_2)$	1.4110		1.4129
$R(C_1-H_4)$	1.0905		1.0904
$R(C_1-H_5)$	1.0994		1.0988
$\angle(H_4-C_1-H_6)$	109.1874		109.3356
$\angle(H_4-C_1-O_2)$	107.3419		107.2258
$\angle(H_5-C_1-H_6)$	108.6363		108.7766
$\angle(H_5-C_1-O_2)$	111.2216		111.0692
$\angle(C_1-O_2-C_3)$	110.7703		111.2271
$R(C_{10}-O_{11})$		1.1700	1.1698
$\angle(O_{11}-C_{10}-O_{12})$		180.0000	178.0606
$R(C_{10}-O_2)$			2.8120
$\angle(C_1-O_2-C_{10})$			124.3933
$\angle(O_{11}-C_{10}-O_2)$			90.9712

[a] Bond lengths are in angstroms, and bond angles are in degrees.

TABLE 2: MP2/6-311++G(d,p) Vibrational Data for DME, CO_2, and DME·CO_2

		monomer		complex		
	assignmentn	freq.[a]	int.[b]	freq.[a]	int.[b]	shift[a]
CH_3OCH_3	$\nu_1^{DME}(a_1)$	3185.0	21.3	3187.8	18.2	2.8
	$\nu_2^{DME}(a_1)$	3028.3	65.4	3033.5	70.4	5.2
	$\nu_3^{DME}(a_1)$	1541.6	1.7	1541.5	1.3	−0.1
	$\nu_4^{DME}(a_1)$	1507.7	0.4	1507.4	0.3	−0.3
	$\nu_5^{DME}(a_1)$	1283.1	6.1	1286.4	5.9	3.3
	$\nu_6^{DME}(a_1)$	968.6	40.5	966.9	49.0	−1.7
	$\nu_7^{DME}(a_1)$	422.8	1.8	423.2	2.8	0.4
	$\nu_8^{DME}(a_2)$	3091.0	0.0	3099.9	0.0	8.9
	$\nu_9^{DME}(a_2)$	1498.0	0.0	1500.0	0.0	2.0
	$\nu_{10}^{DME}(a_2)$	1177.3	0.0	1178.6	0.0	1.3
	$\nu_{11}^{DME}(a_2)$	198.6	0.0	200.7	0.0	2.1
	$\nu_{12}^{DME}(b_1)$	3184.4	26.6	3187.2	16.3	2.8
	$\nu_{13}^{DME}(b_1)$	3020.3	53.9	3026.2	48.7	5.9
	$\nu_{14}^{DME}(b_1)$	1521.8	12.9	1521.6	15.5	−0.2
	$\nu_{15}^{DME}(b_1)$	1482.1	3.4	1481.7	0.3	−0.4
	$\nu_{16}^{DME}(b_1)$	1225.3	103.1	1223.7	95.2	−1.6
	$\nu_{17}^{DME}(b_1)$	1138.9	27.7	1138.9	27.2	0.0
	$\nu_{18}^{DME}(b_2)$	3086.0	119.3	3094.3	106.7	8.3
	$\nu_{19}^{DME}(b_2)$	1508.4	13.5	1510.6	13.6	2.2
	$\nu_{20}^{DME}(b_2)$	1212.4	8.1	1213.8	8.5	1.4
	$\nu_{21}^{DME}(b_2)$	261.9	6.8	261.7	6.0	−0.2
CO_2	$\nu_1^{CO_2}(a_1)$	1335.4	0.0	1338.1	0.3	2.7
	$\nu_{2a}^{CO_2}(a_1)$	655.2	24.7	643.1	49.7	−12.1
	$\nu_3^{CO_2}(b_1)$	2432.7	603.9	2435.0	541.4	2.3
	$\nu_{2b}^{CO_2}(b_2)$	655.2	24.7	660.1	22.6	4.9
van der Waals modes				119.8	0.0	
				80.9	0.2	
				42.5	6.3	
				41.5	0.7	
				38.6	0.0	

[a] Frequencies in cm^{-1}. [b] Intensities in km mol^{-1}.

TABLE 3: Observed Infrared Frequencies, in cm^{-1}, and Complexation Shifts, in cm^{-1}, for CO_2, DME, and DME·CO_2

	$\nu_{complex}$	$\nu_{monomer}$	$\Delta\nu$
$\nu_1+\nu_3(^{12}CO_2)$	3701.5	3703.5	−2.0
$\nu_1+\nu_3(^{13}CO_2)$	3620.1	3622.8	−2.7
$2\nu_2+\nu_3(^{12}CO_2)$	3589.6	3601.0	−11.4
$2\nu_2+\nu_3(^{13}CO_2)$	3499.5	3515.4	−15.7
$\nu_1^{DME},\nu_{12}^{DME}$	2998.6	2994.5	4.1
$2\nu_3^{DME}$	2938.3	2936.6	1.7
$\nu_3+\nu_{19}$(DME)	2933.8	2932.0	1.8
ν_{18}^{DME}	2921.8	2919.8	2.0
$2\nu_{14}^{DME}$	2918.0	2916.0	2.0
$\nu_{14}+\nu_{19}$(DME)	2910.3	2908.6	1.7
$2\nu_{19}^{DME}$	2892.8	2889.7	3.1
$\nu_3+\nu_{15}$(DME)	2888.6	2883.2	5.4
$\nu_{14}+\nu_{15}$(DME)	2872.8	2870.1	2.7
$\nu_{15}+\nu_{19}$(DME)	2869.3	2868	1.7
$\nu_{2\ ^{12}CO_2}^{DME},\nu_{13}^{DME}$	2818.6	2814.7	4.3
$\nu_{3\ ^{13}CO_2}$	2340.5	2341.8	−1.3
ν_3	2275.1	2276.0	−0.9
$\nu_6+\nu_{16}$(DME)	2091.8	2095.5	−3.7
$\nu_6+\nu_{17}$(DME)	2019.5	2023.0	−3.5
ν_5^{DME}	1248.5	1246.2	2.3
ν_6^{DME}	928.4	930.6	−2.2
$\nu_{2a}^{^{12}CO_2}$	668.8	664.3	4.5
$\nu_{2b}^{^{12}CO_2}$	650.2	664.3	−14.1
$\nu_{2a}^{^{13}CO_2}$	649.8	645.5	4.3
$\nu_{2b}^{^{13}CO_2}$	632.0	645.5	−13.5

also be seen that the fundamentals of the complex, where applicable, are described by their Herzberg number in the monomer, with the monomer given as a superscript. Also given are the complexation shifts $\Delta\nu$, defined as $\nu_{complex} - \nu_{monomer}$. Although many of the shifts are quite small, several of them are sufficiently large to be experimentally observable.

Vibrational Spectra. In spectra of mixed DME/CO_2 solutions in LAr, several new bands were detected that are absent in the spectra of single monomer solutions. These signal the formation of a complex between DME and CO_2. Their frequencies are compared with the corresponding monomer frequencies in Table 3. The observations are illustrated in Figure 2, the three panels of which show relevant spectral regions in more detail. The spectra were recorded from solutions containing mole fractions of 1×10^{-4} for DME and 4×10^{-5} for CO_2.

Figure 2A gives the region of the CO_2 bending modes. In the monomer, these modes are degenerate, as is clear from the lower trace. With decreasing temperature, two new bands are seen to develop in the spectrum of the mixed solution, one blue shifted by 4.5 cm^{-1} and the other red shifted by 14.1 cm^{-1}. The obvious lifting of the degeneracy is in agreement with the calculations, where shifts of +4.9 and −12.1 cm^{-1} are predicted, in good agreement with observations. A similar splitting was observed in the matrix infrared spectra of H_2O·CO_2.[2] We assign the observed bands according to the predictions, with the bending localized in the heavy atom plane of the complex, $\nu_{2a}^{CO_2}(a_1)$, blue shifted from the monomer band. The lifting of the degeneracy is also observed for the DME·$^{13}CO_2$. Table 3 shows that the observed complexation shifts are slightly smaller than for the normal complex, in line with expected isotope effects. The middle panel of Figure 2 gives the region of the antisymmetric CO_2 stretch, $\nu_3^{CO_2}(b_1)$. For the monomer, trace b, a relatively broad, symmetric band is found at 2348.1 cm^{-1}. For the mixed solution, the observed band, shown in trace a, is asymmetric and its maximum appears at lower frequency. This suggests the presence of a slightly red shifted complex band.

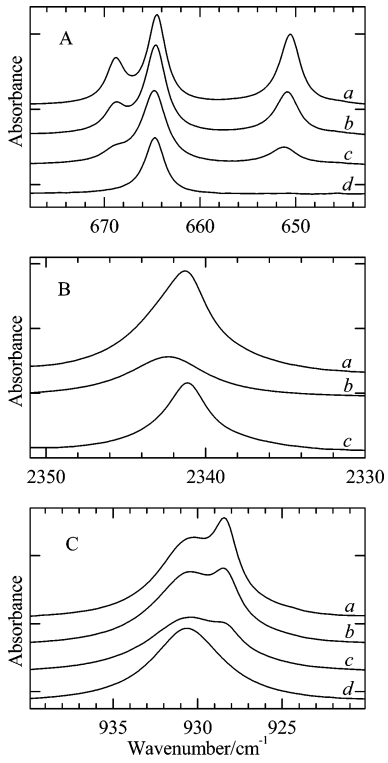

Figure 2. Infrared spectra of DME and CO_2 in LAr. A. Region of $\nu_2^{CO_2}$, recorded at 97 K: (a) mixture of DME and CO_2 in LAr; (b) CO_2 in LAr; (c) spectrum due to the complex, obtained by subtracting the CO_2 contribution from trace a. The tick mark interval on the vertical axis equals 0.5 absorbance units. B. The region of $\nu_1^{CO_2}$: (a−c) a mixture of DME and CO_2 in LAr at 97, 105 and 117 K, respectively; (d) solution of CO_2 at 97 K. The tick mark interval on the vertical axis equals 0.1 absorbance units. C. The region of ν_6^{DME}: (a−c) a mixture of DME and CO_2 in LAr at 97, 105, and 117 K, respectively; (d) solution of DME at 97 K. The tick mark interval on the vertical axis equals 0.5 absorbance units.

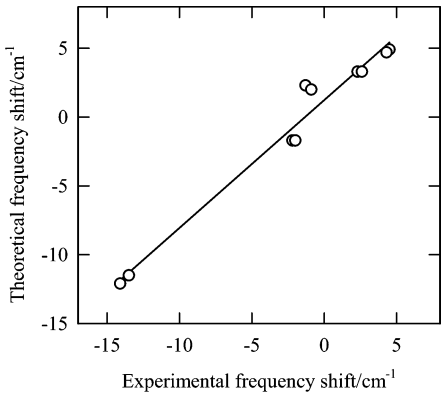

Figure 3. Comparison of ab initio with observed complexation shifts for vibrational modes of DME·CO_2. The solid line is the linear regression curve.

The latter was isolated by subtracting out the monomer contribution and is shown in trace c. It is found to be *red* shifted by 1.3 cm^{-1}, in contradiction with the ab initio calculations, which predict a *blue* shift of 4.1 cm^{-1} for this mode; for the complex using $^{13}CO_2$, the experimental and theoretical shifts are −0.9 and +2.0 cm^{-1}, respectively. To put this in the context of the behavior of the other bands of the same complex, in Figure 3, we have plotted the observed complexation shifts for a number of fundamentals, in abscissa, against their ab initio value, in ordinate. In view of the Fermi resonances in the CH_3 stretching region, these modes were not used in this graph, as

were the complex bands assigned to overtones and combination bands, because for the latter obviously the predicted values are missing. Figure 3 reveals a reasonable correlation between the two sets of data. The linear regression line, shown as the solid line, was calculated using all points shown in the graph: it does not pass through the origin. It can be seen that this must be mainly due to the $\nu_3^{CO_2}$ data. The regression line allows small positive theoretical shifts to be correlated with small negative experimental shifts. However, the position of the regression line is obviously influenced by the rather strongly deviating $\nu_3^{CO_2}$ points: when these points are deleted from the regression, the new line still does not pass exactly through the origin but is much closer to it, making the deviation of the $\nu_3^{CO_2}$ points even more pronounced. The reasons for this are not yet understood.

Panel C of Figure 2 gives the region of $\nu_6^{DME}(a_1)$ and serves to show that also for the dimethyl ether moiety complex bands are observed. The spectra show the complex band emerging with increasing intensity at lower temperatures, on the low-frequency side of the monomer band. Its shift from the latter is -2.2 cm^{-1}, in the same direction but slightly larger than the corresponding ab initio shift in Table 2.

In the CH_3 stretching region of the spectrum of a monomer DME solution, a complicated pattern is observed in which no less than 12 transitions can be distinguished, whereas only 5 allowed fundamentals must be assigned. Previous studies on DME, refs 31−37 and references therein, converge on the assignment of $\nu_1^{DME}(a_1)$ and $\nu_{12}^{DME}(b_1)$ to the highest band in this region, at 2994.5 cm^{-1}, and of $\nu_2^{DME}(a_1)$ and $\nu_{13}^{DME}(b_1)$ to the lowest band in this region, at 2814.7 cm^{-1}. This grouping of the fundamentals suggests weak interaction between the modes in different methyl groupings, which is confirmed by the ab initio results in Table 2. The assignments of $\nu_{18}^{DME}(b_2)$ in the same literature are less consistent, but a frequency in the 2920 cm^{-1} area appears to be the more generally accepted. In Table 3, we have adopted these assigments, with the remaining bands tentatively assigned to overtones or combination bands, enhanced by Fermi resonance with the methyl stretch fundamentals,[38] of the methyl deformations observed in the monomer at 1477 ($\nu_3^{DME}(a_1)$), 1459 ($\nu_{14}^{DME}(b_1)$, 1457 ($\nu_{19}^{DME}(b_2)$), and 1428 cm^{-1} ($\nu_{15}^{DME}(b_1)$).

For the mixed DME/CO_2 solutions in the CH_3 stretching region, a series of complex bands were detected as shoulders on the monomer bands. Spectral subtraction techniques were used to accurately measure their complexation shifts. The data in Table 3 indicate that these fall in the 0−5 cm^{-1} interval. The Fermi resonances present in this region, which are not accounted for in the harmonic ab initio frequencies in Table 2, prevent a meaningful comparison between the two sets of data.

The stoichiometry of the complex was determined in the usual way,[39] by inspecting the linearity of the correlation, throughout a series of spectra recorded isothermally from solutions with varying momomer concentrations, of the intensity of a complex band with the product of appropriate powers of the intensities of a monomer DME and a monomer CO_2 band. The powers were chosen to represent 1:1, 1:2, and 2:1 stoichiometries. The complex bands at 928, 668, and 650 cm^{-1} were analyzed in combination with the 931 (DME) and 664 cm^{-1} (CO_2) monomer bands. Band areas obtained from least squares band fittings of the spectra were used as integrated intensities. The degree of linearity in each case was expressed as the χ^2 value of the linear regression between the two sets of data. The χ^2 values obtained have been collected in Table 4. It can be seen that the value for the 1:1 complex is at least 6 times smaller than for the other stoichiometries, which ensures that the bands investigated are due to a complex with stoichiometry DME·CO_2. A qualitative comparison shows that throughout our temperature and concentration studies the intensity variations of the other bands correlate closely with those of the bands used in the above analysis, so that it may be concluded that no complexes with other stoichiometries have been detected.

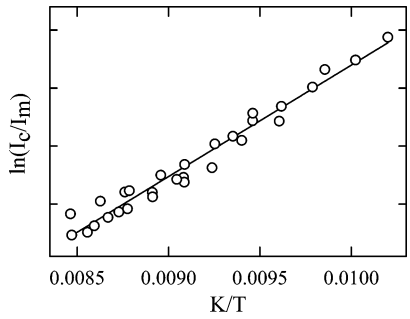

Figure 4. Van't Hoff plot for the temperature study of mixtures of DME and CO_2 in LAr. The solid line is the linear regression curve.

TABLE 4: χ-Square Values of the Stoichiometry Analysis of the DME/CO_2 Complex

stoichiometry	928 cm^{-1}	668 cm^{-1}	650 cm^{-1}
1:1	1.1×10^{-5}	4.2×10^{-4}	1.1×10^{-3}
1:2	8.2×10^{-4}	2.7×10^{-3}	9.0×10^{-3}
2:1	1.3×10^{-4}	7.4×10^{-3}	2.1×10^{-2}
2:2	8.6×10^{-4}	2.8×10^{-3}	7.6×10^{-3}

TABLE 5: Entropies and Enthalpies of Solvation

	DME	CO_2	DME·CO_2
$\Delta_{sol}S°$/J mol^{-1} K^{-1}	−92(2)	−63(2)	−127(2)
$\Delta_{sol}H°$/kJ mol^{-1}	−23.5(2)	−16.8(3)	−33.9(3)

Stability of the Complex. The standard complexation enthalpy difference $\Delta_{LAr}H°$ for the reaction between DME and CO_2 in liquid argon was derived using the Van't Hoff isochore. The latter establishes a linear relation, with a slope related to $\Delta_{LAr}H°/R$[23,40] between the inverse temperature and $\ln(I_{AB}/I_A\times I_B)$, in which I_A, I_B, and I_{AB} are the intensities of a band of monomers A and B and of the complex AB, respectively. For the present complex, the intensities were measured in spectra of mixed solutions containing mole fractions between 1×10^{-4} and 2×10^{-4} in DME and between 2×10^{-5} and 4×10^{-5} in CO_2, recorded at different temperatures between 97.0 and 117.0 K. Band areas of the 934 and 664 cm^{-1} bands were used as monomer intensities, whereas for the complex, the sum of the band areas of the 668 and 650 cm^{-1} bands was used. The band areas were obtained as described in the previous paragraph. The Van't Hoff plot constructed using the data from several temperature runs is shown in Figure 4, with the resulting linear regression line shown in solid. The slope of this line, corrected for temperature variations of the density of the solution as described before,[23,40] yielded a $\Delta_{LAr}H°$ of −8.0(3) kJ mol^{-1}.

The experimental value of $\Delta_{LAr}H°$ is substantially lower than the ab initio complexation energies, but it should be realized that they are quite different quantities. To put the two results in the proper perspective, we have transformed the complexation enthalpy in LAr into a gas-phase complexation energy. In a first step, the solvent influence on the enthalpy was removed using Monte Carlo calculations. In these, the solute/solvent interactions were modeled using Lennard-Jones and polarization terms, as described before.[41] The solvation enthalpies and entropies derived from these calculations have been collected in Table 5. The solvation influence on the complexation enthalpy is easily derived from these data, resulting in a solvent-

destabilization of the complex by −6.4(3) kJ mol^{-1}. The $\Delta_{LAr}H°$ combined with this solvent-destabilization results in a gas-phase enthalpy of −14.4(5) kJ mol^{-1}. In the next step, the thermal and zero-point contributions were removed from $\Delta_{gas}H°$ by straightforward statistical thermodynamics, using ab inito structures and vibrational frequencies to calculate rotational and vibrational terms.[42] It was found that this results in a correction by 2.1 kJ mol^{-1}, so that the complexation energy is derived to be −16.5(5) kJ mol^{-1}. This value is slightly larger than the MP2/6-311++G(d,p) ab initio result but is in very good agreement with the value of the single-point MP2/6-311++G(3df,2pd) value of −15.58 kJ mol^{-1}. This is taken to indicate that at the latter level the residual basis set incompleteness error has become very small.

Fermi Resonance in the CO_2 Moiety. The anharmonic interaction between the E_g^+ sublevel $|0,2^0,0\rangle$ of the doubly excited bending mode, and the E_g^+ symmetric stretching $|1,0,0\rangle$ state in vapor phase CO_2 gives rise to the prototypal, but infrared forbidden, example of a Fermi resonance. In DME·CO_2, the degeneracy of the bending is lifted, giving rise to an a_1 and a b_1 normal coordinate. Their $v = 2$ levels $2\nu_{2a}^{CO_2}$ and $2\ \nu_{2b}^{CO_2}$ both have a_1 symmetry, which is also the symmetry of the first excited level of the CO_2 symmetric stretching mode. Hence, depending on the proximity of the levels, in the complex, Fermi resonances with both first overtones of the deformations may occur. A further complication may arise for the $2\nu_{2a}^{CO_2}$ and $2\ \nu_{2b}^{CO_2}$ levels: the vibrational quantum numbers of these states fulfill the requirements for a Darling Dennison resonance. The lack of experimental evidence from similar CO_2 complexes, however, makes it very difficult to aniticipate on the importance of this type of resonance, the more so because no quartic force field is available for the complex.

In contrast with monomeric CO_2, the transitions from the ground state to the levels involved in the complex are infrared allowed and should, at least in principle, be observable. In view of the very small ab initio intensity for $\nu_1^{CO_2}$ in Table 2, it must be expected, however, that unless significant contributions from, for instance, electrical anharmonicity are present the components of the Fermi doublets will be quite weak. The region in which these transitions occur is well-known and was carefully investigated in our infrared spectra, using solutions that were nearly saturated in DME and CO_2, with the solutions contained in a 7 cm path length cell. The resulting spectra, recorded at 90 K, are shown in Figure 5, for experiments using CO_2 with natural isotopic abundances as well as $^{13}CO_2$.

For the ^{12}C isotopomer, Figure 5 compares the spectrum of the DME/CO_2 solution, trace a, with the DME solution, trace b. In the frequency range shown, a CO_2 solution with a concentration similar to the one used for trace a exhibits a spectrum with a horizontal baseline. It may be remarked that this contrasts with the spectra described by M. Bulanin et al.,[43,44] in which interaction-induced transitions were observed in this spectral region. The absence of such bands in our spectra is explained by the fact that in Bulanin's study the spectra were recorded at much higher path lengths and with much higher concentrations of CO_2 in the more polarizable solvents krypton and xenon. The comparison of trace a with trace b reveals that the weak bands at 1382 and 1321 cm^{-1} must be assigned to the DME/$^{12}CO_2$ complex. The weakness of these bands is illustrated by the ratio of the integrated intensity of the 650 cm^{-1} $\nu_{2b}^{CO_2}$ complex band to that of the 1382 cm^{-1} band, which was found by least squares band fitting to be 235(30). A transition corresponding to the 1382 cm^{-1} band was reported, and assigned to the symmetric CO_2 stretch, by Fredin et al.[2] at 1384.5 cm^{-1} for H_2O·CO_2. These authors, however, did not observe a transition corresponding to the 1321 cm^{-1} band. Trace c of Figure 5 gives the spectrum of the DME/CO_2 solution, from which an appropriately rescaled spectrum b has been subtracted, whereas trace d gives the similar spectrum obtained from a DME/$^{13}CO_2$ solution. The shifts of the weak bands in d as compared to c ascertain that they originate from the CO_2 moiety of the complex.

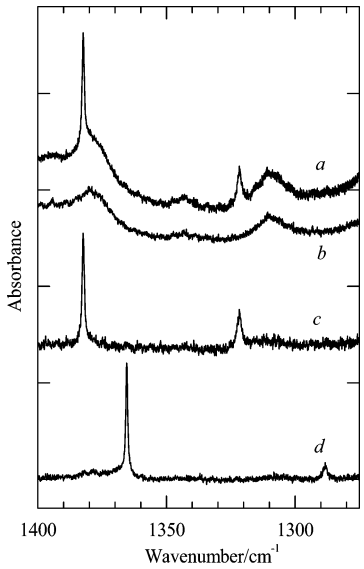

Figure 5. Infrared spectra of DME and CO_2 in LAr, at 97 K, in the region of the $\nu_1^{CO_2}/\nu_2^{CO_2}$ Fermi resonance, recorded at 0.1 cm^{-1} resolution: (a) mixture of DME and CO_2 in LAr; (b) DME in LAr; (c) spectrum due to the complex DME·CO_2, isolated by subtracting trace b from trace a; (d) spectrum due to DME·$^{13}CO_2$, obtained similarly to that in trace c. The tick mark interval on the vertical axis equals 0.01 absorbance units.

Because for either isotopomer only a doublet is observed, it is tempting to conclude that the unperturbed symmetric CO_2 symmetric stretch, $\nu_1^{CO_2}$, is in resonance with only one of the two unperturbed CO_2 bending overtone levels, $2\nu_{2a}^{CO_2}$ or $2\nu_{2b}^{CO_2}$. This, however, is not supported by the ab initio calculations of the cubic force constants k_{122} and $k_{12'2'}$, with "1" standing for $\nu_1^{CO_2}$, "2" for $2\nu_{2a}^{CO_2}$, and "2′" for $2\nu_{2b}^{CO_2}$. When expressed with the help of dimensionless normal coordinates, and using the Nielsen definition,[45] k_{122} equals $2W$.[46] The cubic force field calculations, at the MP2/6-31+G(d) level, result in $k_{122} = 75.0$ cm^{-1}, very close to the ab initio value of the corresponding force constant for monomer CO_2, 75.4 cm^{-1}. The latter, in turn, is in close agreement with the experimental value.[47] The same calculation leads to the sligthly bigger value of 78.5 cm^{-1} for $k_{12'2'}$. This shows that, even with $2\nu_{2b}^{CO_2}$ further away from $\nu_1^{CO_2}$ than $2\nu_{2a}^{CO_2}$, its Fermi resonance with $\nu_1^{CO_2}$ cannot be neglected. Some insight in the influence of the second resonance was gained from a straightforward three-dimensional matrix perturbation calculation, in which the ab initio value for $\nu_1^{CO_2}$ and twice the ab initio values of $\nu_{2a}^{CO_2}$ and $\nu_{2b}^{CO_2}$ were treated as the unperturbed frequencies, and the ab initio cubic force constants k_{122} and $k_{12'2'}$ were used to construct the off-diagonal elements in the usual way.[46] In these calculations, the Darling Dennison resonance between the $2\nu_{2a}^{CO_2}$ and $2\nu_{2b}^{CO_2}$ levels was neglected. In double-resonance (2R) calculations both k_{122} and $k_{12'2'}$ were included, while in single-resonance (1R) calculations $k_{12'2'}$ was equated to zero. In the 2R calculation for the ^{12}C complex, the two highest components of the Fermi triplet were shifted by +10.6 and +8.7 cm^{-1} in comparison with the predictions from

the 1R calculation. For the ^{13}C complex, the 2R versus the 1R calculation yields shifts of +9.0 and +4.6 cm^{-1}. These results emphasize that, assuming the ab initio cubic force constants are an acceptable approximation to the true values, a useful analysis of the observations requires accounting for the second Fermi resonance, which can only be done when the corresponding transition can be located experimentally. It is not unlikely that in the present experiments this band was not observed because it is lost under the much stronger DME band near 1249 cm^{-1} in the monomer as well as in the complex. In that case, matrix isolation, with its significantly reduced bandwidths, would be the preferred method to attempt observation of this band. The mole fractions of monomers used to obtain the spectra in Figure 5 are typical for matrix isolation experiments. The less than optimal signal-to-noise ratio of the spectra, combined with their extensive accumulation time, then makes clear that matrixes would have to be deposited with thicknesses of the same order as the path length of the liquid cell used in this study, i.e., 7 cm. This is unrealistically thick, and therefore, matrix isolation experiments were not pursued. As a consequence, no quantitative analysis of the observed Fermi doublets can be given at this stage.

Conclusions

In this study, the structure and vibrational properties of the 1:1 complex between the Lewis acid carbon dioxide and the Lewis base dimethyl ether was investigated using ab initio calculations at the MP2/6-311++G(d,p). The complex was investigated experimentally, using infrared spectroscopy of solutions in liquid argon. In these solutions, bands due to a complex were identified, with the stoichiometry analysis proving its 1:1 composition. Its stability, measured as the standard complexation enthalpy difference, was found to be 8.0(3) kJ mol^{-1}, which, when extrapolated to an energy difference, was found to be −16.5(5) kJ mol^{-1}, in very good agreement with the BSSE corrected complexation energy derived from single-point MP2/6-311++G(3df,2pd) calculations at the converged MP2/6-311++g(d,p) structures.

Acknowledgment. The authors thank the FWO-Vlaanderen for their assistance toward the purchase of the spectroscopic equipment used in this study. The authors also thank the Flemish Community for financial support through the Special Research Fund (BOF). Dr. Sonia Melikova (Department of Physics, University of St Petersburg) is thanked for useful discussions.

References and Notes

(1) Jacox, M. E.; Milligan, D. E. *Spectrochim. Acta* **1961**, *17*, 1196−1202.
(2) Fredin, L.; Nelander, B.; Ribbegard, G. *Chem. Scripta* **1975**, *7*, 11−13.
(3) Blatchford, M. A. *J. Am. Chem. Soc.* **2002**, *124*, 14818−14819.
(4) Columberg, B.; Bauder, A.; Heineking, N.; Stahl, W.; Makarewicz, J. *Mol. Phys.* **1998**, *93*, 215−228.
(5) Peterson, K. I.; Klemperer, W. *J. Chem. Phys.* **1984**, *80*, 2439−2445.
(6) Vigasin, A. A.; Adiks, T. G.; Tarakanova, E. G.; Yukhnevich, G. B. *J. Quant. Spectrosc. Radiat. Transfer* **1994**, *52*, 295−301.
(7) Kazarian, S. G.; Vincent, M. F.; Bright, F. V.; Liotta, C. L.; Eckert, C. A. *J. Am. Chem. Soc.* **1996**, *118*, 1729−1736.
(8) Reilly, G. T.; Bokis, C. P.; Donohue, M. D. *Intern. J. Thermophys.* **1995**, *16*, 599−610.
(9) Raveendran, P.; Wallen, S. L. *J. Am. Chem. Soc.* **2002**, *124*, 12590−12599.
(10) Bukowski, R.; Szalewicz, K.; Chabalowski, C. F. *J. Phys. Chem. A* **1999**, *103*, 7322−7340.
(11) Falk, M.; Miller, A. G. *Vib. Spectrosc.* **1992**, *4*, 105−108.
(12) Meredith, J. C.; Johnston, K. P.; Seminario, J. M.; Kazarian, S. G.; Eckert, C. A. *J. Phys. Chem. A* **1996**, *100*, 10837−10848.
(13) Tso, T.-L.; Lee, E. K. C. *J. Phys. Chem. A* **1985**, *89*, 1612−1618.
(14) Tso, T.-L.; Lee, E. K. C. *J. Phys. Chem. A* **1985**, *89*, 1648−1631.
(15) Van Der Zwet, G. P.; Allamandola, L. J.; Baas, F.; Greenberg, J. M. *J. Mol. Struct.* **1989**, *195*, 213−225.
(16) Wierzejewdka, M.; Dziadosz, M. *J. Mol. Struct.* **1999**, *513*, 155−167.
(17) Makarewicz, J.; Ha, T.-K.; Bauder, A. *J. Chem. Phys.* **1993**, *99*, 3694−3699.
(18) Nelson, M. R.; Borkman, R. F. *J. Phys. Chem. A* **1998**, *102*, 7860−7863.
(19) Nxumalo, L. M.; Ford, T. A.; Cox, A. J. *J. Mol. Struct.* **1994**, *307*, 153−169.
(20) Zhang, N. R.; Shillady, D. D. *J. Chem. Phys.* **1994**, *100*, 5230−5236.
(21) Jamróz, M. H.; Dobrowolski, J. C.; Bajdor, K.; Borowiak, M. A. *J. Mol. Struct.* **1995**, *349*, 9−12.
(22) Fedotov, A. N.; Simonov, A. P. *Zh. Fiz. Khim.* **1999**, *73*, 1852−1855.
(23) Van der Veken, B. J. In *Low-temperature molecular spectroscopy*; Faust, R., Ed.; Kluwer Academic Publishers: Dordrecht, The Netherlands, 1996; p 371.
(24) Simon, S.; Duran, M.; Dannenberg, J. J. *J. Chem. Phys.* **1996**, *105*, 11024.
(25) Frisch, M. J.; Trucks, G. W.; Schlegel, H. B.; Scuseria, G. E.; Robb, M. A.; Cheeseman, J. R.; Zakrzewski, V. G.; Montgomery, J. A., Jr.; Stratmann, R. E.; Burant, J. C.; Dapprich, S.; Millam, J. M.; Daniels, A. D.; Kudin, K. N.; Strain, M. C.; Farkas, O.; Tomasi, J.; Barone, V.; Cossi, M.; Cammi, R.; Mennucci, B.; Pomelli, C.; Adamo, C.; Clifford, S.; Ochterski, J.; Petersson, G. A.; Ayala, P. Y.; Cui, Q.; Morokuma, K.; Malick, D. K.; Rabuck, A. D.; Raghavachari, K.; Foresman, J. B.; Cioslowski, J.; Ortiz, J. V.; Stefanov, B. B.; Liu, G.; Liashenko, A.; Piskorz, P.; Komaromi, I.; Gomperts, R.; Martin, R. L.; Fox, D. J.; Keith, T.; Al-Laham, M. A.; Peng, C. Y.; Nanayakkara, A.; Gonzalez, C.; Challacombe, M.; Gill, P. M. W.; Johnson, B. G.; Chen, W.; Wong, M. W.; Andres, J. L.; Head-Gordon, M.; Replogle, E. S.; Pople, J. A. *Gaussian 98*, revision A.11; Gaussian, Inc.: Pittsburgh, PA, 1998.
(26) *BOSS*, version 4.1; Jorgensen, W. L., Ed.; Yale University: New Haven, CT, 1999.
(27) Allen, M. P.; Tildesley, D. J. *Computer simulations of liquids*; Oxford University Press: Oxford, 1987.
(28) Levy, R. M.; Gallicchio, E. *Annu. Rev. Phys. Chem.* **1998**, *49*, 531−567.
(29) Herrebout, W. A.; Lundell, J.; Van der Veken, B. J. *J. Phys. Chem. A* **1999**, *103*, 7639−7645.
(30) Herrebout, W. A.; Van der Veken, B. J. In *Vibrational Spectra and Structure*; Durig, J. R., Ed.; Elsevier: Amsterdam, 2003, in press.
(31) Coudert, L. H.; Carçabal, P.; Chevalier, M.; Broquier, M.; Hepp, M.; Herman, M. *J. Mol. Spectrosc.* **2002**, *212*, 203−207.
(32) Goebel, J.; Ault, B. S.; Del Bene, J. E. *J. Phys. Chem. A* **2000**, *104*, 2033−2037.
(33) Barnes, A. J.; Beech, T. R. *Chem. Phys. Lett.* **1983**, *94*, 568−570.
(34) Han, S. W.; Kim, K. *J. Mol. Struct.* **1999**, *475*, 43−53.
(35) Stewart, G.; Ruoff, R.; Kulp, T.; McDonald, J. D. *J. Chem. Phys.* **1984**, *80*, 5353−5358.
(36) Levin, I. W.; Pearce, R. A. R.; Spiker, R. C., Jr. *J. Chem. Phys.* **1978**, *68*, 3471−3480.
(37) Allan, A.; McKean, D. C.; Perchard, J.-P.; Josien, M.-L. *Spectrochim. Acta* **1971**, *27 A*, 1409−1437.
(38) McKean, D. C. *Spectrochim. Acta A* **1973**, *29A*, 1559−1574.
(39) Van der Veken, B. J.; De Munck, F. R. *J. Chem. Phys.* **1992**, *97*, 3060−3071.
(40) Bertsev, V. V.; Golubev, N. S.; Shchepkin, D. N. *Opt. Spektrosk.* **1976**, *40*, 951.
(41) Van der Veken, B. J.; Herrebout, W. A. *J. Phys. Chem. A* **2001**, *105*, 7198−7204.
(42) McQuarrie, D. A. *Statistical Mechanics*; University Science Books: Sausolito, CA, 2000.
(43) Bulanin, M. O.; Granskii, P. V. *Opt. Spektrosk.* **1984**, *57*, 771−773.
(44) Bulanin, M. O.; Granskii, P. V.; Melikova, S. M. *Opt. Spektrosk.* **1986**, *61*, 487−490.
(45) Nielsen, H. H. *The Vibration−rotation energies of molecules and their spectra in the infrared*; Flüge, S.: Berlin, 1959; Vol. XXXVII/1.
(46) Califano, S. *Vibrational states*; John Wiley & Sons: London, 1976.
(47) Suzuki, I. *J. Mol. Spectrosc.* **1968**, *25*, 479−500.